International Journal of Nanomedicine

Dovepress
open access to scientific and medical research

Open Access Full Text Article

ORIGINAL RESEARCH

SN38-loaded <100 nm targeted liposomes for improving poor solubility and minimizing burst release and toxicity: in vitro and in vivo study

This article was published in the following Dove Press journal:
International Journal of Nanomedicine

Yi-Ping Fang[1,2]
Chih-Hung Chuang[3]
Yi-Jhun Wu[1]
Hsin-Che Lin[1]
Yun-Chi Lu[4]

[1]School of Pharmacy, College of Pharmacy, Kaohsiung Medical University, [2]Department of Medical Research, Kaohsiung Medical University Hospital, [3]Department of Medical Laboratory Science and Biotechnology, College of Health Sciences, Kaohsiung Medical University, [4]Graduate Institute of Medicine, Collage of Medicine, Kaohsiung Medical University, Kaohsiung, Taiwan

Background: SN38 (7-ethyl-10-hydroxycamptothecin) is a camptothecin derivative acts against various tumors. However, SN38 is hydrolyzed in the physiological environment (pH 7.4), and this instability interferes with its potential therapeutic effect. Our objective was to investigate SN38-loaded liposomes to overcome the poor solubility of SN38 and its biodistribution, which further diminish its toxicity.

Materials and methods: The sub-100 nm targeted liposomes was employed to deliver SN-38 and evaluate the characterization, release behaviors, cytotoxicity, in vivo pharmacokinetics and biochemical assay.

Results: The SN38-loaded targeted liposomes consisted of small (100.49 nm) spherical nanoparticles with negative charge (–37.93 mV) and high entrapment efficiency (92.47%). The release behavior of the SN38-loaded targeted liposomes was fitted with Higuchi kinetics (R^2=0.9860). Free SN38 presented initial burst release. The IC_{50} for the SN38-loaded targeted liposomes (0.11 μM) was significantly lower than for the SN38 solution (0.37 μM) in the MCF7 cell line ($P<0.01$). Confocal laser scanning microscopy also confirmed highly efficient accumulation in the MCF7 cells. Pharmacokinetics demonstrated that the SN38-loaded targeted liposomes had a slightly increased half-life and mean residence time and decreased area under the concentration–time curve and maximum concentration. The results suggested that retention was achieved while the exposure of SN38 was significantly decreased. A noninvasive in vivo imaging system also showed that the targeted liposomes selectively targeted MCF7 tumors. In vivo toxicity data demonstrated that the decrease in platelets was significantly improved by SN38-loaded targeted liposomes, and diarrhea was not observed in BALB/c mice.

Conclusion: In summary, SN38-loaded targeted liposomes could be a good candidate for application in human breast cancer.

Keywords: SN38, targeted liposome, pharmacokinetics, human breast cancer, toxicity

Introduction

SN38 (7-ethyl-10-hydroxycamptothecin) is a potential anticancer drug. It is an active metabolite of irinotecan that has demonstrated ~100–1,000 times the cytotoxic potency of irinotecan, which is in clinical use.[1] Currently, irinotecan is frequently used in clinical treatment for advanced colorectal cancer, but it causes serious toxicity problems in patients. Only 2%–8% of the irinotecan administered is converted to SN38.[2] To achieve a better therapeutic outcome, the usage dose must be increased, but increased doses are accompanied by serious toxicity problems in patients. Moreover, unpredictable and individual interpatient diversity in the conversion of irinotecan to SN38 is probably due to individual carboxylesterase activity in plasma.[3] The administration of low-dose

Correspondence: Yi-Ping Fang
School of Pharmacy, College of Pharmacy, Kaohsiung Medical University, 100 Shih-Chuan First Road, San Ming, Kaohsiung 80708, Taiwan
Tel +886 7 312 1101 ext 2261
Fax +886 7 321 0683
Email ypfang@kmu.edu.tw

submit your manuscript | www.dovepress.com
Dovepress
http://dx.doi.org/10.2147/IJN.S158426

SN38 can simultaneously minimize the toxicity and achieve better therapeutic outcomes.

The investigation of SN38 for preclinical study requires overcoming several limitations. The structural backbone of the series of camptothecin analogues, including SN38, contains five rings, and an α-hydroxy-δ-lactone ring moiety (E-ring) plays a major functional role. When SN38 is hydrolyzed in the physiological environment (pH 7.4) or under basic conditions, the lactone ring is opened to yield a carboxylate form, making SN38 nonfunctional.[4,5] Research has highlighted that the lactone ring of SN38 is stable at pH ≤4.5 and hydrolyzes completely to the carboxylate form at pH 9.0.[6] The instability of SN38 in physiological circulation is a major hurdle in its development, as the therapeutic effect of SN38 is prevented by its conversion to the carboxylate form. SN38 is a small molecule (molecular weight 392.4 Da), but its poor water solubility (11–38 μg/mL) and high partition coefficient (log P 2.65) limit its ability to dissolve in water or most pharmaceutically approved solvents. This has obstructed development of parenteral formulations.[6–8] Moreover, SN38 includes camptothecin derivatives, which still present toxicity problems. The principal dose-limiting toxicity observed is delayed diarrhea, with or without neutropenia. Myelosuppression is also the second-most commonly encountered toxicity of irinotecan.[9]

Multiple strategies have been investigated to ameliorate these drawbacks by chemical modification or via nanomedicine approaches.[10] Among these strategies, three candidates have been approved for various stages of clinical trials. EZN2208, which is in a Phase I trial, has a four-arm polyethylene glycol (PEG) conjugation at the C20 position of SN38 to increase water-solubility and decrease diarrhea, although neutropenia has also occurred in patients.[11] NK012, now in a Phase II study, has hydrophilic PEG bound via a hydrophobic polyglutamate linker at the C10 position of SN38. It self-assembles into micelles in aqueous solution.[12] However, side effects, including grade 3 and 4 neutropenia and leukopenia, still occur.[13] Liposome-encapsulated (LE) SN38 uses a liposomal formulation to carry SN38, and as of 2016 a Phase II trial was studying how well liposomal SN38 works in the treatment of metastatic colorectal cancer.[14] Various carriers have also been investigated, including such polymers as polylactide-*co*-glycolic acid nanoparticles,[15] poly-hydroxypropyl methacrylamide,[16] chitosan,[17] a polymer decorated with hyaluronic acid,[18] a conjugated phospholipid,[19] dextran,[20] and a conjugated antibody.[21] Moreover, immunomedicine has brought precise and individual therapies in recent decades. IMMU132 (sacituzumab govitecan) is an antibody–drug conjugate for the treatment of metastatic triple-negative breast cancer. IMMU132 has been submitted for accelerated approval. Due to the lack of tumor-factor biomarkers for specific diseases, the development period is longer. From unmet clinical need, rapid drug research and development is one of the strategies.[22,23]

Liposomal formulations are a well-established technique in drug-delivery systems, and some were approved two decades ago. Since SN38 is unstable at physiological pH, the use of a liposomal structure can protect the drug against hydrolysis and achieve high stability. SN38 entrapped by a liposomal bilayer can avoid direct contact with the blood, increasing its safety. Evidence has indicated that the blood concentration of PEGylated liposomes is significantly higher than that of conventional liposomes.[24] Clinically, the main problem that remains in cancer treatment is the destruction of cancerous cells and healthy cells simultaneously. Studies have indicated that folate receptors are overexpressed on the vast majority of cancer tissue, while their expression is limited in healthy tissue and organs. Moreover, several folate-conjugated nanomedicine systems could provide targeting effects in specific cells.[25]

The aim of this study was to investigate SN38-loaded liposomes of lower particle size and higher entrapment efficiency to overcome the poor solubility of SN38, improve targeting against breast cancer, and diminish side effects. The formulation was initially characterized and evaluated, and in vitro release and kinetics were assayed. An in vitro cellular assay was performed to investigate cytotoxicity and cellular uptake. Pharmacokinetics and noninvasive in vivo imaging system (IVIS) analyses were performed to understand the effects on SN38 localization and targeting. Complete blood cell counts and biochemistry assays were performed to obtain information on systemic toxicity.

Materials and methods

Chemicals and reagents

SN38, Hoechst 33258, cholesterol, Pluronic F68, rhodamine B, and phosphotungstic acid were purchased from Sigma-Aldrich (St Louis, MO, USA). DSPE (1,2-distearoyl-*sn*-glycero-3-phosphoethanolamine and 1,2-distearoyl-*sn*-glycero-3-phosphoethanolamine–*N*-(folate[polyethylene glycol 2,000) ($PEG_{2,000}$ folate) were purchased from Avanti Polar Lipids (Alabaster, AL, USA). Epikuron 200 was obtained from Lucas Meyer (Champlan, France). Sodium hydroxide, phosphoric acid, disodium hydrogen phosphate dehydrate, and sodium dihydrogen phosphate monohydrate were obtained from Merck (Darmstadt, Germany). Methanol, ethanol, and acetonitrile of analytical reagent grade were obtained from Mallinckrodt (Staines-upon-Thames, UK). The human breast adenocarcinoma cell line MCF7 was purchased from the Culture Collection and Research Center of the Food Industry Research and Development Institute (Hsinchu, Taiwan).

High-performance liquid chromatography analysis of SN38

SN38 was analyzed by high-performance liquid chromatography (HPLC). The HPLC system consisted of an L-2130 pump, L-2200 autosampler, L-7420 ultraviolet-visible detector at 265 nm (Hitachi, Tokyo, Japan), and a Purospher Star RP-18 column (250×4.6 mm, internal diameters 5 μm; Merck). The mobile phase was a mixture of 25 mM sodium dihydrogen phosphate (NaH_2PO_4, adjusted to pH 3.1 by 85% phosphoric acid) and acetonitrile (50:50 v:v), and the flow rate was 1 mL/min. Limits of detection and quantitation of SN38 were determined by dissolving SN38 at decreasing concentrations in distilled deionized water until the signal:noise ratios were 3 and 10, respectively. The linearity of the standard curves and intraday and interday precision and accuracy were established.

Preparation of <100 nm targeted liposomes

SN38 was encapsulated in liposomes using the thin-film method. In brief, the lipid phase and SN38 were dissolved in 95% ethanol, the mixture evaporated by a rotary evaporator at 60°C, and residual solvents removed under nitrogen for 10 minutes. The film was hydrated with distilled deionized water at pH 3.4 (adjusted with 10% phosphoric acid). Coarse liposomes were dispersed by a probe sonicator (digital Sonifier 250; Branson, Danbury, CT, USA) at 30 W for 10 minutes. Then, liposomes were sequentially extruded through 0.4 μm, 0.2 μm, and 0.1 μm polycarbonate membrane filters for five cycles each with a miniextruder. Fine liposomes were obtained and stored at 4°C.

Particle size and ζ-potential

Average particle diameter and ζ-potential of the liposomes were measured by laser light scattering with a helium–neon laser at 630 nm (Zetasizer 3000HSA; Malvern Instruments, Malvern, UK). The polydispersity index (PDI) was also used to measure size distribution. All liposomes were diluted 100-fold with distilled deionized water to measure the count rate. The determination was repeated three times per sample for three samples.

Encapsulation efficiency

LE SN38 was separated from the unencapsulated (free) portion by ultracentrifugation. Fresh liposomes were centrifuged at 120,000 rpm (771,000 *g*) for 1 hour at 4°C in a Hitachi CS150 GXL ultracentrifuge. The supernatant was collected to quantify the unencapsulated drug. The original fresh liposomes (50 μL) were mixed with chloroform (50 μL) and methanol (900 μL) by vortexing for 1 minute and then centrifugation at 12,000 rpm for 10 minutes at 4°C to determine the total drug load. Drug-entrapment efficiency was calculated:

$$\text{Entrapment efficiency (\%)} = \frac{\text{Concentration}_{\text{total}} - \text{Concentration}_{\text{free}}}{\text{Concentration}_{\text{total}}} \times 100\%$$

Morphology

Liposome morphology was observed by transmission electron microscopy (TEM) to characterize the microstruce. The liposome suspension was dropped onto a Formvar/carbon film on a 200-mesh copper grid (FCF-200-Cu; Electron Microscopy Sciences, Hatfield, PA, USA) and stained with 1% phosphotungstic acid for 20 minutes. After the negative-staining process, the sample was washed with distilled deionized water. The water was vacuumed out overnight, and the sample was then observed using TEM (JEM-2000EX II; JEOL, Tokyo, Japan).

In vitro release study

An in vitro release study was performed by the dialysis method. Dialysis bags with a molecular-weight cutoff of 6,000–8,000 Da (pore size 1.8 nm; Orange Scientific, Braine-l'Alleud, Belgium) were soaked with distilled deionized water for 12 hours before the experiment. Dialysis bags containing SN38-loaded liposome or SN38 solution were subsequently incubated in flasks containing 15 mL medium (PBS:ethanol 1:1 v:v) in a 37°C water bath. At appropriate intervals, 500 μL aliquots of the medium were withdrawn for analysis and immediately replaced with an equal volume of fresh medium. Release kinetics were investigated using different models, including zero-order, first-order, and Higuchi kinetics. Correlation coefficients and each release equation were calculated from the respective plots.

Cytotoxicity assay

MCF7 cells were incubated in MEM with 10% FBS and 1% antibiotics in a humidified atmosphere containing 5% CO_2/95% air at 37°C. MCF7 cells were seeded on 96-well culture plates at a cell density of 10^5 cells/well. After overnight incubation, the medium was replaced with fresh medium containing SN38 solution or SN38-loaded liposomes at final concentrations of 0.1, 0.5, 5, and 10 μM for 48 hours. Cells were washed with PBS and reacted with 10 μL CCK-8

(Dojindo, Kumamoto, Japan) for 3 hours. The absorbance was read at 450 nm by an enzyme-linked immunosorbent-assay reader (BioTek Epoch; Thermo Fisher Scientific, Waltham, MA, USA) to determine the quantity of surviving cells. IC_{50} was calculated using a four-parameter logistic function standard curve analysis of the dose response.

Flow cytometry

The uptake of SN38-loaded liposomes by MCF7 was investigated using flow cytometry (FACScan; BD Biosciences, San Jose, CA, USA). Incorporated rhodamine B was used as the fluorescence indicator. MCF7 cells were seeded into six-well plates at 10^6 cells per well and allowed to adhere overnight. The medium was removed and replaced with fresh medium containing SN38-loaded liposomes at final concentrations of 0.5, 5, and 10 μM for 4 hours. MCF7 cells were lysed with TrypLE™ (Thermo Fisher Scientific) and neutralized with medium. The mixture was centrifuged at 800 rpm for 5 minutes and the supernatant removed. Then, cell pellets were washed twice with PBS and cells suspended in PBS and analyzed by flow cytometry. The fluorescence signal was read with a 488 laser by the FACScan.

Confocal laser scanning microscopy

Confocal laser scanning microscopy (CLSM) images were used to evaluate the uptake and intracellular distribution of SN38-loaded liposomes into MCF7 cells. Rhodamine B was used as the fluorescence indicator. MCF7 cells were seeded in six-well chambered cover glass at 10^6 cells/well in complete cell-culture media. The medium was removed and the cells treated with SN38-loaded liposomes at final concentrations of 0.5, 5, and 10 μM for 0.5, 2, and 4 hours. The treatment medium was removed and cells were washed twice and then fixed in 4% paraformaldehyde for 10 minutes at room temperature. Fixed cells were then rinsed twice with PBS and stained with Hoechst 33258 (5 μg/mL) for 10 minutes. Cells were again washed twice with PBS and then flushed with mounting medium (Ibidi GmbH, Munich, Germany). Images were then taken using a CLSM (FV1000; Olympus, Tokyo, Japan). Rhodamine was observed at an excitation wavelength of 570 nm and emission wavelength of 590 nm, and Hoechst was observed at an excitation wavelength of 350 nm and emission wavelength of 450 nm.

Animals

In vivo pharmacokinetic and cancer-targeting exams were performed in healthy male BALB/c mice and BALB/c nude mice (6–8 weeks old) obtained from the Laboratory Animal Center of the National Science Council, Taipei, Taiwan. All animal experiments were conducted in accordance with institutional guidelines and approved by the Animal Care and Use Committee of Kaohsiung Medical University, Kaohsiung, Taiwan. All animals were starved overnight prior to the experiments.

In vivo pharmacokinetics and biodistribution

BALB/c mice were anesthetized by halothane vapor with a vaporizer system. Mice in the control group were administered SN38 dissolved in dimethyl sulfoxide solution, and the liposome group was administered SN38-loaded microsomes, each intravenously injected with doses of 10 mg/kg. At time intervals of 20 minutes, 40 minutes, and 1, 2, 4, and 6 hours, 60–70 μL blood samples were collected in heparin-containing tubes (Vacutainer; BD, Franklin Lakes, NJ) and immediately centrifuged at 12,000 rpm for 10 minutes. The plasma was collected and stored at −20°C. Mice were killed at the final time point, heart, liver, spleen, lungs, kidneys, stomach, intestines, rectum, muscle, and feces collected, washed with PBS, and stored at −20°C.

SN38 in plasma was then analyzed. Plasma samples (180 μL) were mixed with 20 μL 300 μL/mL internal standard solution, and 360 μL acetonitrile was added to induce protein precipitation. The mixture was centrifuged at 12,000 rpm for 10 minutes and the supernatant evaporated under vacuum. The final dry residue was resuspended in the mobile phase and analyzed by HPLC. Organs were homogenized in 1 mL PBS at 17,800 rpm for 30 seconds. Then, following the same process, homogenized organs were mixed with internal standard solution and acetonitrile and analyzed by HPLC.

Correlation coefficients for the pharmacokinetic compartmental model were calculated and predicted using WinNonlin software (version 5.3; Certara, Princeton, NJ, USA). The area under the concentration–time curve ($AUC_{0-\infty}$) was calculated by the trapezoidal rule. Half-lives of the distribution phase ($t_{½\alpha}$) and elimination phase ($t_{½\beta}$) and the clearance (Cl) were also obtained. The Cl value was calculated as dose/$AUC_{0-\infty}$, and mean residence time (MRT) and volume of distribution at a steady state (V_{ss}) were obtained by summation of the central and tissue compartments.

In vivo cancer targeting

To investigate targeting ability, two human breast cancer cell lines were tested in the study. The cell lines MDA-MB468 and MCF7 were purchased from the American Type Culture

Collection. Cells were cultured in DMEM (Sigma-Aldrich) supplemented with 10% heat-inactivated bovine calf serum, 100 units/mL penicillin, and 100 mg/mL streptomycin at 37°C in a humidified atmosphere of 5% CO_2.

Nude BALB/c nude mice bearing established MDA-MB468 or MCF7 tumors (50–100 mm^3) at the mammary gland were anesthetized by halothane vapor with a vaporizer system and then intravenously injected with 500 µM rhodamine-loaded liposomes. Optical images were sequentially obtained at 2 hours with the IVIS spectrum-imaging system (PerkinElmer, Waltham, MA, USA). The fluorescence intensities were analyzed with Living Imaging version 4.2 (PerkinElmer) analysis software.

Biochemical analysis

Blood was collected in test tubes containing heparin anticoagulant for complete blood count (CBC) analysis. Blood was analyzed for number of erythrocytes, platelets (Plt), and total white blood cells using an automated blood analyzer (XT-1800i; Sysmex, Kobe, Japan). The hemoglobin, red blood cells and hepatic function were also analyzed. Reference values were obtained from Charles River Laboratory.[26] ALT and AST were also evaluated.

Statistical analysis

Statistical analyses were performed using the unpaired Student's *t*-test with Winks SDA 6.0 software (TexaSoft, Cedar Hill, TX, USA). Analysis of variance was also performed. Subgroup comparisons were performed using Newman–Keuls multiple comparisons. A 0.05 level of probability was used as the level of significance. All data are expressed as the means ± SD.

Results

Characterization of SN38-loaded liposomes

We compared three kinds of liposomes: conventional, stealth, and targeted (Figure 1). Table 1 compares the particle size, ζ-potential, and entrapment efficiency of these kinds of liposomes. Conventional liposomes consisted of Epikuron 200 and cholesterol. Particles were 72.5 nm in diameter with 0.097 PDI, ζ-potential of –4.2 mV, and 79% entrapment efficiency. When the liposome was decorated with DSPE-$PEG_{2,000}$ (stealth) or DSPE-$PEG_{2,000}$ folate (targeted), particle size and PDI increased to 100 nm and 0.22–0.26, respectively. The ζ-potential increased to –46 to –37 mV and entrapment efficiency to 82%–92%. SN38-loaded targeted liposomes were transparent and showed nanometer-sized sphericity by TEM (Figure 2).

Release behavior

In vitro release of SN38 from solution and from SN38-loaded liposomes was performed using the dialysis method. A pH 7.4 buffer was used to simulate body fluid, but SN38 has poor solubility in the pH 7.4 buffer medium. To obtain evidence regarding release behavior, the selection of a suitable dialysis medium is an important factor. Research has demonstrated that SN38 is insoluble in most class 3 solvents (less toxic solvents); it was solubilized only in dimethyl sulfoxide and formic acid at 0.5% (w:w). To enhance the solubility of

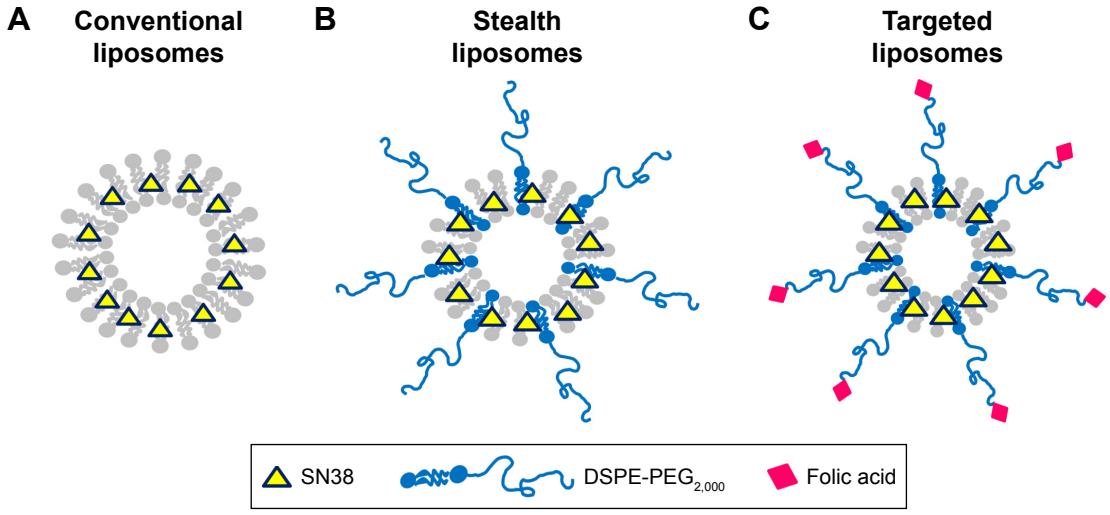

Figure 1 SN38 loaded in various liposomes.
Note: (**A**) Conventional liposome, (**B**) stealth liposome, and (**C**) target liposome.
Abbreviations: DSPE, 1,2-distearoyl-*sn*-glycero-3-phosphoethanolamine; PEG, polyethylene glycol.

Table 1 Characterization of SN38 loaded in various liposomal formulations

	Particle size (nm)	Polydispersity index	ζ-potential (mV)	Encapsulation efficiency (%)
Conventional liposomes	72.5±0.6	0.097±0.005	−4.2±0.6	79.13±1.61
Stealth liposomes	103.47±1.02	0.260±0.03	−46.80±1.56	82.67±0.55
Targeted liposomes	100.49±0.91	0.223±0.02	−37.93±2.87	92.47±2.95

Note: Data shown as means ± SD (n=3).

SN38 and achieve sink conditions, ethanol was added to the incubation medium at a final concentration of PBS:ethanol 1:1 (v:v).[27,28] Release profiles and correlation coefficients of SN38 solution and SN38-loaded liposomes were investigated, as shown in Table 2. The cumulative release percentage data were plotted and fitted based on three mathematical models: zero-order, first-order, and Higuchi. The SN38 solution showed a biphasic release pattern with an initial burst release of 80% within 2 hours, followed by saturation at 24 hours. In terms of liposome-release behavior, there was no significant difference among the release patterns of SN38-loaded basic, stealth, and targeted liposomes ($P>0.05$). SN38-loaded basic, stealth, and targeted liposomes were all best fitted by the Higuchi model, with R^2=0.9933, 0.9458, and 0.9860, respectively. Moreover, the rate constants of SN38 solution and SN38-loaded basic, stealth, and targeted liposomes were 18.94, 6.8776, 7.4988, and 8.3034, respectively.

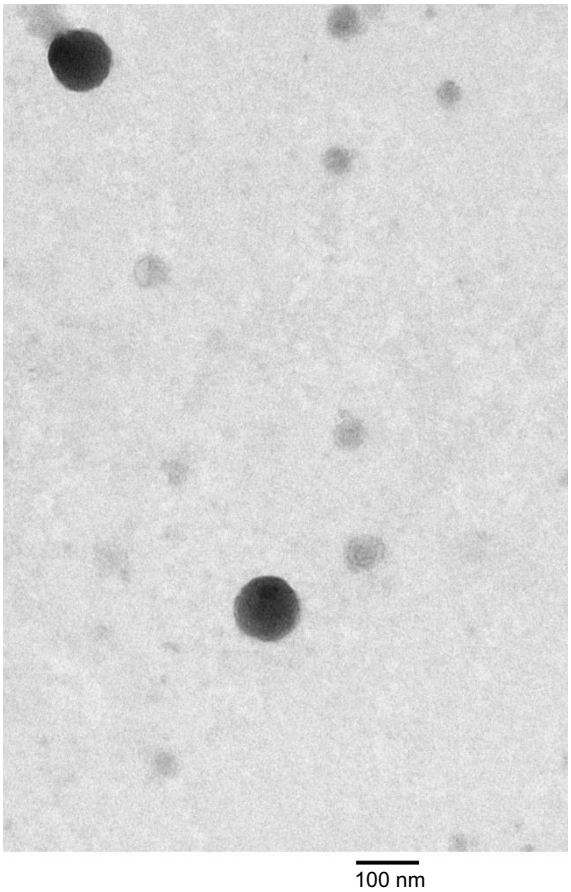

Figure 2 Transmission electron microscopy of SN38-loaded targeted liposomes.
Note: Magnification (×100 k) at 75 kv.

In vitro cytotoxicity assay

In vitro cytotoxic activities of the SN38 solution and SN38-loaded stealth or targeted liposomes were examined, as shown in Figure 3. In all cases, there was a linear correlation (R^2=0.8621–0.9540) between cytotoxicity and drug concentration in the medium within the tested range (0.1–10 μM). Moreover, the addition of 0.5 μM SN38 with targeted liposomes significantly reduced the cell viability of MCF7 to 19% of that in the SN38 solution group ($P<0.05$). The addition of 10 μM SN38-loaded targeted liposomes significantly decreased cell viability to 0 ($P<0.05$). In addition, we observed that when SN38-loaded stealth liposomes were incubated at low concentrations (0.1, 0.5 μM), there were no significant differences in results using the SN38 solution. At higher concentrations (5, 10 μM), cell viability was decreased to 12% and 4%, respectively. As shown in Table 3, IC_{50} values for SN38-loaded targeted liposomes (0.11 μM) were significantly lower than those of SN38 solution (0.37 μM) and SN38 with stealth liposomes (0.36 μM) in the MCF7 cell line ($P<0.01$). Moreover, the IC_{50} values of SN38-loaded targeted liposomes decreased to 70% of those of the SN38 solution.

Analysis of tumor uptake via flow cytometry and CLSM

To understand the uptake of SN38-loaded targeted liposomes, flow cytometry and CLSM analysis were performed using rhodamine B as a fluorescence marker. Flow cytometry of SN38-loaded targeted liposomes is shown in Figure 4. MCF7 cells treated with different concentrations of SN38-loaded targeted liposomes showed increased fluorescence intensity ($P<0.05$). CLSM was also used to visualize the targeting effect of SN38-loaded targeted liposomes, as shown in Figure 5. Confocal images of the MCF7 cells treated with

Table 2 Mathematical models and coefficients for the in vitro release of SN38 in various liposomal formulations

	Zero-order $Q=k$	First-order $Q=1-e^{-kt}$	Higuchi model $Q=kt^{1/2}$
SN38 solution	$y=2.7458x+52.4098$ $R^2=0.5744$	$y=0.0372x+3.9819$ $R^2=0.2212$	$y=18.94x+29.274$ $R^2=0.6182$
Conventional liposomes	$y=1.2948x+5.1478$ $R^2=0.9456$	$y=0.0875x+1.8591$ $R^2=0.6649$	$y=6.8776x-1.3447$ $R^2=0.9933$
Stealth liposomes	$y=8.5846x+1.3232$ $R^2=0.8649$	$y=0.0718x+2.2596$ $R^2=0.5829$	$y=7.4988x+0.9384$ $R^2=0.9458$
Targeted liposomes	$y=1.6193x+4.2072$ $R^2=0.9759$	$y=0.1008x+1.7876$ $R^2=0.6858$	$y=8.3034x-3.2722$ $R^2=0.9860$

Notes: Data shown as means ± SD (n=3). Correlation coefficients and release-rate equations calculated from slopes of respective plots. *Q*, fraction of drug released at time *t*; *k*, release constants.

SN38-loaded targeted liposomes for 0.5, 2, and 4 hours showed the accumulation of red in the cells. Moreover, the accumulated amount was time-dependent.

In vivo pharmacokinetics and biodistribution

To investigate the pharmacokinetic behavior of SN38-loaded targeted liposomes in circulation in vivo, their plasma concentration was measured for 6 hours. We established that limits of detection and quantitation for SN38 were 5 and 10 ng/mL, respectively. The linear range in plasma was 0.1–20 μg/mL (R^2=0.9999). The pharmacokinetics and tissue distribution of SN38 solution and SN38-loaded targeted liposomes were tested in BALB/c mice following a single intravenous bolus-dose administration at the 10 mg/kg dose level. The profile of the mean plasma concentration of SN38 vs time is shown in Figure 6. There was no significant difference in plasma concentration observed after the administration of SN38 solution and SN38-loaded targeted liposomes. Furthermore, the pharmacokinetic parameters were predicted by WinNonlin. The pharmacokinetics of SN38 in solution or loaded into the targeted liposomes were best fitted by a two-compartment model based on the lower Akaike information criterion and higher values (R^2=0.9999). Table 4 summarizes the pharmacokinetic parameters after an intravenous bolus of SN38 in solution or SN38-loaded targeted liposomes for 6 hours. The SN38 solution and SN38-loaded targeted liposomes showed markedly different maximum concentration C_{max} of 29.02±1.22 and 44.69±1.36 μg/mL, respectively ($P<0.001$). Moreover, V_{ss} values for the SN38-loaded targeted liposomes (0.99±0.18 L/kg) were significantly higher than that obtained without this formulation (0.54±0.16 L/kg) ($P<0.001$).

After intravenous administration of SN38 solution or SN38-loaded targeted liposomes, organs and tissue were homogenized and the SN38 extracted. The linear range in each tissue was 0.01–1 μg/mL (R^2=0.9914–0.9983), with a good linear relationship. As shown in Figure 7, the organ distribution of SN38-loaded targeted liposomes showed significant accumulation in the liver, spleen, and lung compared with accumulation in the nonformulation group ($P<0.05$). However, no significant differences ($P>0.05$) between the accumulation of SN38 administered in solution and the accumulation of SN38-loaded targeted liposomes were observed in lower-perfusion organs, such as the stomach, intestine, and muscle. Six hours after administration, SN38-loaded targeted liposomes were detected at different levels in different tissue

Table 3 IC_{50} values of different SN38-loaded liposomal formulations in MCF7 after 48 hours' treatment

	IC_{50} (μM)
	MCF7
SN38 solution	0.37±0.02
SN38-loaded stealth liposomes	0.36±0.03
SN38-loaded targeted liposomes	0.11±0.02**

Notes: Data shown as means ± SD (n=6). **$P<0.01$ compared to SN38 solution.

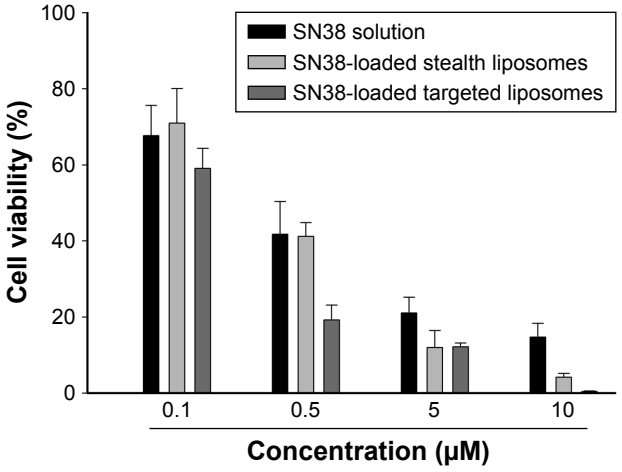

Figure 3 Cytotoxicity of various liposomes in the MCF7 cell line.
Note: Data shown as means ± SD (n=6).

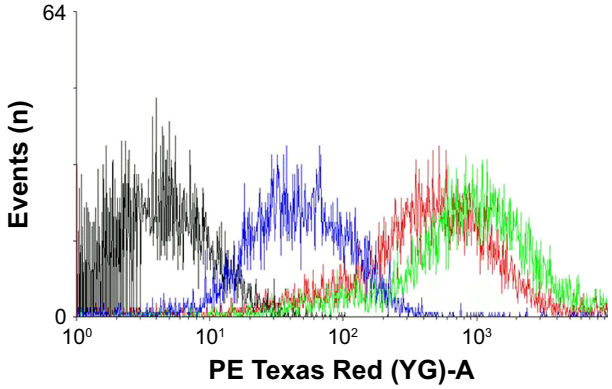

Figure 4 Flow-cytometry measurement of SN38-loaded targeted liposome uptake by MCF7 cells after treatment with 0.5, 5, and 10 μM in final concentration for 4 hours.

in the order lung > spleen > liver > kidney > heart. The highest C_{max} of 2.71±0.73 μg/g was found in the lungs.

In vivo cancer targeting

To investigate whether targeted liposomes could selectively target MCF7 tumors in vivo, mice bearing established MDA-MB468 and MCF7 tumors (50–100 mm^3) at the mammary gland were intravenously injected with 500 μM rhodamine-loaded targeted liposomes. The fluorescence intensities of the mice were recorded with the IVIS at 30, 60, and 120 minutes after injection. Imaging analysis revealed that the fluorescence signal of the rhodamine-loaded targeted liposomes in the MCF7 tumors was stronger than that in the MDA-MB-468 tumors, as shown in Figure 8.

In vivo toxicity assessment

BALB/c mice were administered a single dose of 10 mg/kg SN38 in solution or in targeted liposomes and killed after 6 hours. A summary of CBC and in vivo biochemistry-assay data is shown in Table 5. The blank (untreated) group showed no significant difference from reference values of BALB/c mice. CBC data showed that after treatment with SN38 solution, slight increases in hemoglobin and red blood cell counts were observed in comparison to the reference values. Hematocrit and Plt values were significantly decreased to 32.13%±6.45% and 197.33%±69.43×10^9/L, respectively,

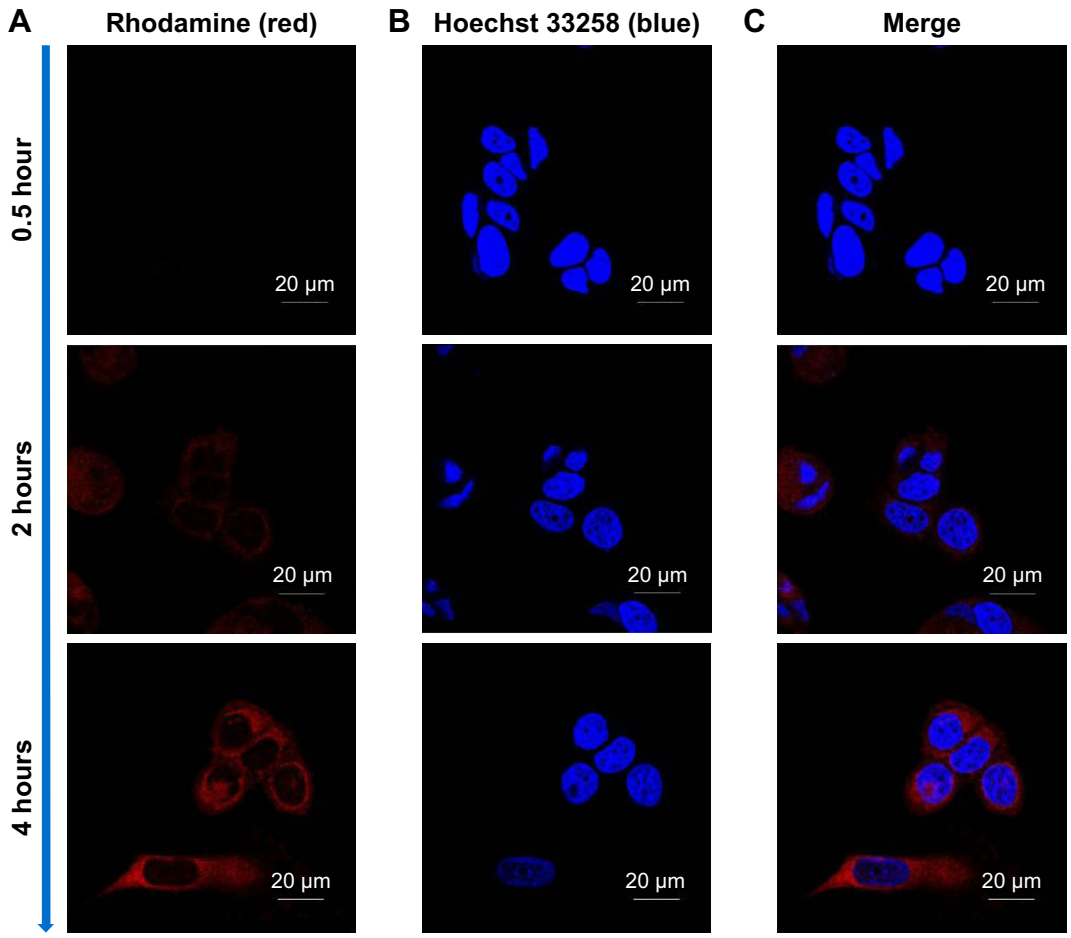

Figure 5 Confocal laser scanning microscopy of uptake of SN38-loaded targeted liposome in MCF7 cells after treatment for 0.5, 2, and 4 hours.
Notes: (**A**) Rhodamine channels showing red fluorescence from liposomes distributed; (**B**) Hoechst 33258 channels showing blue fluorescence from Hoechst 33258-stained nuclei; (**C**) merged channels of liposomes (red) localized at MCF7 cells (blue). Magnification 1,000×.

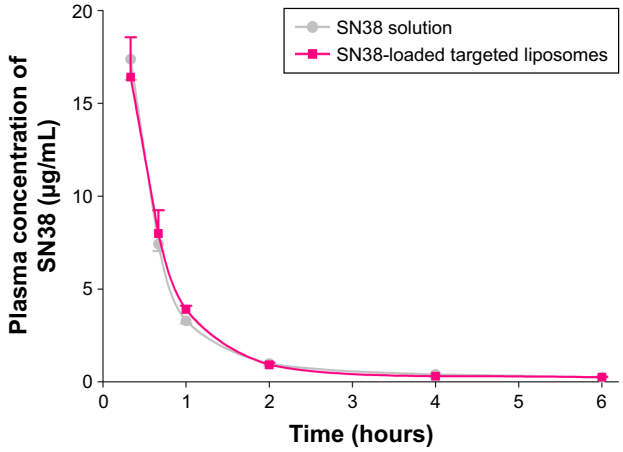

Figure 6 In vivo plasma concentration of SN38 vs time profiles of SN38 with/without targeted liposomes in BALB/c mice after IV 10 mg/kg bolus administration of dosage.
Note: Data shown as mean ± SD (n=6).
Abbreviation: IV, intravenous.

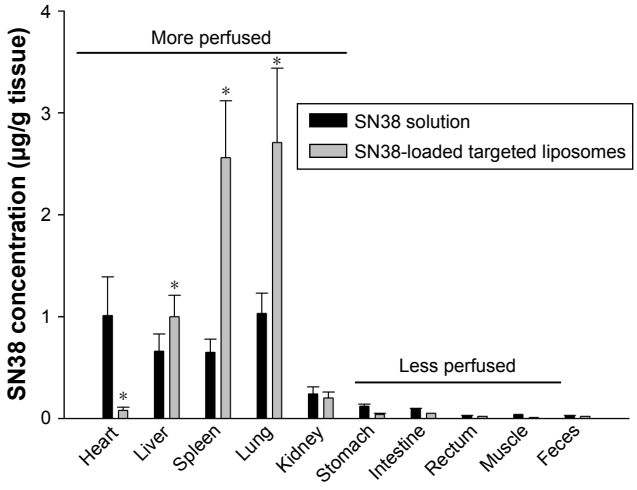

Figure 7 In vivo biodistribution of SN38 solution or SN38-loaded targeted liposomes (10 mg/kg SN38) in BALB/c mice after IV bolus administration via the tail.
Notes: Data shown as mean ± SD (n=6). *$P<0.05$ compared to SN38 solution.
Abbreviation: IV, intravenous.

compared with their reference values. Biochemistry data showed that after treatment with SN38 solution, ALT and AST levels significantly increased in comparison with reference values to 568.33±62.36 and 966.00±58.89 U/L, respectively. In contrast, no changes in white blood cells, lymphocytes, monocytes, or granulocytes were observed 6 hours after the administration of SN38-loaded targeted liposomes. CBC and biochemistry data after SN38-loaded targeted liposome treatment showed similar trends to those after treatment with SN38 solution. In particular, the Plt level greatly increased to 347.00±23.59×10^9/L with SN38-loaded targeted liposome treatment, in contrast to after treatment with SN38 solution. In the SN38-loaded targeted liposome group, Alt levels decreased to 138.67±23.71, approximately equal to the reference values (41–131 U/L).

Discussion

The development of SN38 has been hindered by its poor solubility, instability at physiological pH, and toxicity problems.

Table 4 Comparison of pharmacokinetic parameters of SN38 solution and SN38-loaded targeted liposome after intravenous administration at dosage of 10 mg/kg to BALB/c mice

	SN38 solution	SN38-loaded targeted liposomes
AUC (μg/h/L)	19.60±0.81	14.85±0.63*
$t_{1/2}$ (hours)	0.30±0.02	0.35±0.02
C_{max} (μg/mL)	44.69±1.36	29.02±1.22**
Cl (L/h/kg)	0.51±0.02	0.67±0.03
MRT (hours)	1.07±0.35	1.48±0.32
V_{ss} (L/kg)	0.54±0.16	0.99±0.18**

Notes: Data shown as means ± SD (n=6). *$P<0.05$, **$P<0.001$ compared with SN38 solution.
Abbreviations: AUC, area under curve; $t_{1/2}$, half-life; C_{max}, maximum concentration; Cl, clearance; MRT, mean residence time; V_{ss}, steady-state volume.

This work has revealed SN38-loaded targeted liposomes that both solve the poor-solubility problem and prevent its easy hydrolysis in the physiological environment. the SN38-loaded targeted liposomes were <100 nm spherical nanoparticles with high entrapment efficiency, and also presented lower IC_{50} against MCF7 cell lines than SN38 in solution. Pharmacokinetic results suggested that the SN38 targeted liposomes increased retention but significantly decreased the exposure of SN38. IVIS images indicated that SN38-loaded targeted liposomes selectively targeted MCF7 tumors. In vitro release behavior showed that the targeted liposomes minimized the burst effect, and in vivo results showed that they diminished the toxicity problems of SN38.

Conventional liposomes are significantly smaller than decorated liposomes ($P>0.05$), mainly due to high-molecular-weight decorations, such as DSPE-$PEG_{2,000}$ or DSPE-$PEG_{2,000}$ folate on the outer shell of the liposomes, which increase the particle size. Moreover, conventional, stealth, and targeted liposomes showed significant differences in ζ-potential ($P<0.05$). With no stealth or targeted ligand modifiers, conventional liposomes are nearly unchargeable. The negative charges on liposomes were mainly contributed by DSPE decorations. pKa (most acidic) and pKa (most basic) values of SN38 were 9.68 and 3.91, respectively. In the incorporation of SN38 at pH 3.4, the majority consisted of undissociated molecules, and thus the heightened lipophilicity of SN38 assisted in entrapping it in the phospholipid bilayer of liposomes and achieved higher entrapment efficiency. Research also demonstrated that SN38 is ionized at low and high pH (pKa 1.4 and 8.6) and is significantly more soluble when ionized.[29]

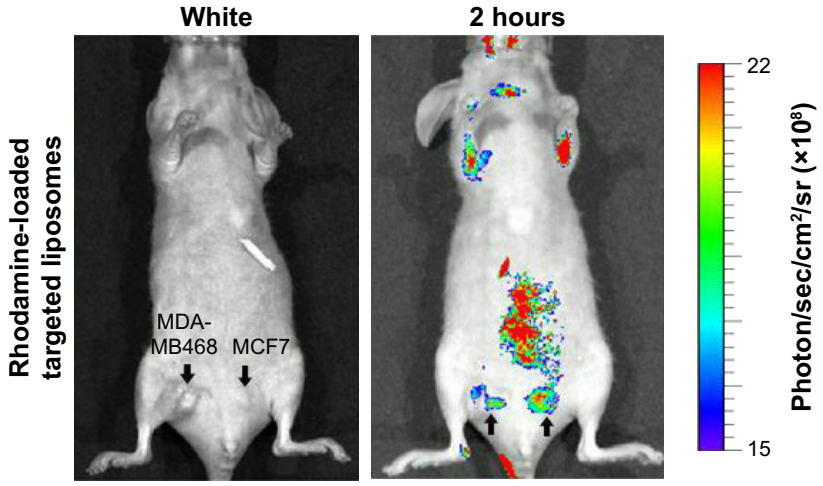

Figure 8 In vivo cancer targeting of targeted liposomes.
Notes: Mice bearing established MDA-MB468 and MCF7 tumors were injected with 500 μM rhodamine-loaded targeted liposomes. Fluorescence intensity in mice recorded on a noninvasive in vivo imaging system (IVIS) 2 hours after injection.

In the liposome-design concept, Epikuron is the main matrix. Cholesterol is incorporated to avoid drug leakage from liposomes, and the exterior is modified with DSPE-$PEG_{2,000}$ or DSPE-$PEG_{2,000}$ folate to prolong in vivo circulation. As main components of the cellular membrane, phospholipids have excellent biocompatibility.[30] In addition, phospholipids are renowned for their amphiphilic structures. The amphiphilicity endows phospholipids with self-assembly, emulsifying, and wetting characteristics. DSPE-$PEG_{2,000}$ is a PEGylated phospholipid used widely in various preparations, and the PEG layer usually serves as a steric barrier to stabilize the molecule.[31] DSPE-$PEG_{2,000}$ folate is linked with folate moiety, which could provide targeting ability.[25]

One of the disadvantages of SN38 is its toxicity. Therefore, precise control of SN38 therapeutic concentration during the therapeutic window could minimize side effects. We aimed to formulate liposomes with a stable release pattern to achieve an effective therapeutic concentration. Based on the release data, unformulated SN38 showed an initial rapid release of almost 80% within 2 hours. The early burst-release phase of SN38 contributed to the low interaction between SN38 and the vehicle itself. Moreover, passive diffusion determined by the concentration gradient was the major driving force.[32] The marked initial burst-release effect would cause the drug quickly to enter the blood circulation and various organs. Higher blood concentrations are clinically

Table 5 Complete blood count and liver function assays of SN38 solution and SN38-loaded targeted liposomes in BALB/c mice after intravenous bolus administration

	Blank[#]	SN38 solution	SN38-loaded targeted liposomes	Reference values
Complete blood count				
WBC count (10^9/L)	5.83±2.20	5.00±1.39	5.20±0.30	3.48–14.03
Lym (%)	81.80±3.12	68.40±12.05	60.97±1.10	48.81–83.19
Mon (%)	5.83±1.11	7.90±2.85	8.23±0.81	3.29–12.48
Gra (%)	12.37±2.14	23.70±10.14	30.80±1.90	9.97–45.86
Hb (g/dL)	16.10±0.44	10.27±1.91*	11.03±1.36*	12.6–20.5
Hct (%)	52.13±1.36	32.13±6.45*	34.50±4.06*	42.1–68.3
RBC count (10^{12}/L)	9.95±0.27	6.21±1.14*	6.64±0.86*	6.93–12.24
Plt count (10^9/L)	586.67±30.11	197.33±69.43**	347.00±23.59**	420–1,698
Liver function markers				
ALT (U/L)	127.00±20.42	568.33±62.36**	138.67±23.71**	41–131 (U/L)
AST (U/L)	165.33±44.11	966.00±58.89**	412.33±60.21**	55–352 (U/L)

Notes: Data shown as means ± SD (n=3). [#]Before intravenous administration in each mouse; *$P<0.05$, **$P<0.001$ compared to blank group.
Abbreviations: WBC, white blood cell; Lym, lymphocyte; Mon, monocyte; Gra, granulocyte; Hb, hemoglobin; Hct, hematocrit; RBC, red blood cell; Plt, platelet.

dangerous, especially in cases of high toxicity, such as that of SN38.

SN38-loaded conventional liposomes and those with stealth or targeted shell decorations were fitted with Higuchi kinetics, and correlation coefficients were high: 0.9458–0.9933. The results indicated that SN38 was loaded into the liposomes, that the drug-release process was based on Fick's law of diffusion, and that the process was dependent on the square root of time. Moreover, the rate constant of SN38 without liposomes (18.94) was significantly higher than that of SN38-loaded conventional, stealth, and targeted liposomes (6.8776, 7.4988, and 8.3034). The rate constant of a carrier's release reflects the properties of the barrier domain within the carrier.[33] For SN38-loaded conventional liposomes or stealth and targeted liposomes, there was high affinity between the drug solute and the lipid bilayer of the carrier. This affinity was reflected in the high entrapment-efficiency data. The sustained-release behavior was also attributed to the incorporation of cholesterol. Research has reported slow drug-release behavior to be characteristic of a rigid liquid-ordered liposome.[34] When a high amount of cholesterol is present in the liposome, the lipid bilayer should be in a rigid liquid-ordered phase and thus enable a prolonged drug-release pattern. For SN38-loaded conventional, stealth, or targeted liposomes, the rate constant clearly shows a slower-release tendency. This result may indicate that the stealth or targeted liposome shell reflects the ordered-chain region of the phospholipid bilayer.

Conventional chemotherapeutic agents lack specificity, and thus an increase in dose is a common strategy; however, this can lead to serious toxicity problems.[35] SN38 is a potential chemotherapeutic agent against various cancer cell lines. If the toxicity problem of SN38 could be reduced, therapeutic outcomes would improve. In this study, SN38 showed marginal cytotoxicity (IC_{50}=0.37 μM) in the MCF7 cell line. Higher concentrations of SN38 decreased the cell viability of MCF7 to 15%, which suggested that SN38 treatment alone can cause obvious cytotoxicity. For SN38-loaded targeted liposomes, we found that at the low SN38 concentration of 0.5 μM, cell viability greatly decreased to 19%. This effect on cell viability suggested that the targeted liposomes had high cytotoxicity toward MCF7 at lower concentrations. Moreover, the IC_{50} of SN38-loaded targeted liposomes was significantly lower than that of SN38 solution (0.37 μM) in the MCF7 cell line ($P<0.01$). These results indicated that SN38-loaded targeted liposomes inhibited MCF7 cells more effectively than the unformulated SN38. In contrast, the SN38-loaded stealth liposomes showed no significant decrease in cytotoxicity or IC_{50} at lower concentrations. Importantly, this finding shows that the concentration of SN38 was a predominant factor influencing cytotoxicity, even of the stealth-decorated liposomes. The cytotoxicity of stealth-decorated liposomes was limited at lower concentrations of SN38, ie, a higher concentration of SN38 resulted in efficacious cytotoxicity, but would cause severe toxicity problems. Therefore, a suitable liposome carrier designed considering not only stealth but also targeting could minimize the concentration of SN38 in clinical use.

Rhodamine, a hydrophobic fluorescent molecular probe, is an excellent tool for determining liposome-particle retention in cells for bioassays.[36,37] According to the flow-cytometry results, SN38-loaded liposomes decorated with folate ligand were taken up by MCF7 cells. Moreover, the uptake relationship was concentration-dependent. Folate receptors are overexpressed in various tumors, and have been targeted in several cancer-therapy studies.[38–40] Moreover, to confirm the uptake of SN38-loaded targeted liposomes by MCF7 cells and understand the mechanism, CLSM techniques were also used, and results were consistent with the flow-cytometry findings. Red fluorescence intensity was clearly observed in MCF7 cells after treatment with SN38-loaded targeted liposomes at a final concentration of 10 mM. This finding indicated that SN38 liposomes with folate modification increased cellular uptake efficiency and targeting specificity in MCF7 cells, despite the relatively low level of folate receptor in MCF7 cells. Moreover, the red florescence probe was incorporated into the lipid bilayer of the SN38-loaded targeted liposomes to show liposome-particle localization in the cell. Based on the CLSM images, we confirmed good uptake of SN38-loaded targeted liposomes by MCF7 cells, with a high degree of accumulation in the nuclei.

Both SN38 solution and SN38-loaded targeted liposomes can be typically described by a two-compartment model. Pharmacokinetic parameters demonstrated that SN38-loaded targeted liposomes prolonged the half-life of SN38 in the bloodstream, but the difference from the results SN38 solution was not significant. These results indicated that PEGylation or targeting modification help vesicles increase circulation time, but the ability to escape mononuclear phagocytic system (MPS) uptake was limited. On the other hand, the biodistribution results showed that for either SN38 solution or SN38-loaded targeted liposomes, the concentration of SN38 accumulated greatly in the well-perfused organs, such as the heart, liver, spleen, lung, and kidney. In contrast, SN38 was rarely found in the stomach, intestine, rectum, and muscle, which are more poorly perfused. The phenomena

match the two-compartment model, in which the drug rapidly enters the central compartment, often followed by the peripheral compartment. To summarize the pharmacokinetic behavior, the SN38-loaded targeted liposomes showed slight increases in half-life and MRT and decreases in AUC and C_{max}, suggesting that retention was achieved but the exposure of SN38 significantly decreased.

The biodistribution results showed higher accumulation in the well-perfused organs, as assumed by the two-compartment model, whose behavior was similar to that of past studies. SN38 was found in significant quantities in the liver and spleen after treatment with SN38-loaded targeted liposomes in comparison with after treatment with unformulated SN38. Pal et al reported that LE SN38 was found mainly in the central compartment organs, with almost no accumulation in peripheral tissue.[41] We discuss this behavior herein. The ζ-potential of SN38-loaded target liposomes (−37.93 mV) was negative, and studies have shown that negatively charged liposomes have a shorter half-life in the bloodstream than neutral liposomes.[42,43] Moreover, a recent review noted that negatively charged phospholipids can be quickly eliminated from the circulatory system and focused on the MPS.[30] However, we assumed that ζ-potential did not play a predominant role in in vivo pharmacokinetic behavior, whereas particle size, composition, and surface decoration were more important. Evidence indicates that the MPS uptake of liposomes by the liver is likewise size-dependent.[44] In the case of this study, the SN38-loaded targeted liposomes were approximately <100 nm in size, which was sufficient to avoid liver uptake. As such, we found that the liver accumulation of SN38-loaded targeted liposomes was clearly lower than the accumulation in the spleen or lung. However, the organ distribution was not strong evidence. A further reason was contributed by PEGylation. PEGylated vesicles strongly reduce MPS uptake, prolong blood circulation, and improve biodistribution in well-perfused tissues.[45]

Irinotecan and topotecan are both used in clinical practice. Common side effects include diarrhea, nausea, and vomiting, while severe effects include leukopenia, neutropenia, and liver dysfunction.[46] Myelosuppression (bone-marrow suppression) is a severe side effect leading to systemic toxicity in camptothecin analogues. In order to understand the administration period, CBC and liver function were monitored. In the case of SN38, Plt were significantly decreased ($P<0.01$) in comparison with levels in the blank group, and the reference value suggested that the type of myelosuppression was closely related to Plt. SN38-loaded targeted liposomes significantly improved this decrease in Plt. Overall, both ALT and AST levels increased significantly compared with those of the blank group, indicating some degree of influence on liver-function markers. After treatment with SN38-loaded targeted liposomes, ALT levels were similar to reference values, but still showed a mildly increased tendency. AST levels were also decreased after treatment with SN38 solution, but remained higher than reference values. Changes in liver-function results reflected that SN38-loaded targeted liposomes to some extent decreased inflammation or toxicity in the liver, since the organ distribution showed lower accumulation in the liver. In addition, both early and delayed diarrhea are the most common results of SN38 toxicity. Previous research has demonstrated that the accumulation of SN38 in the intestine is responsible for diarrhea in a nude mouse model.[47] In this study, diarrhea was not observed in the BALB/c mice. Moreover, limited SN38 concentrations were found in intestines or feces.

Conclusion

SN38 was successfully prepared in targeted liposomes, which simultaneously solved both the poor-solubility problem and the problem of easy hydrolysis in a physiological environment. The resulting SN38-loaded targeted liposomes were spherical under TEM with a well-distributed particle size <100 nm. SN38-loaded targeted liposomes presented much lower IC_{50} than unformulated SN38 against MCF7 cell lines in an in vitro culture study. SN38-loaded targeted liposomes exhibit a release pattern described by Higuchi kinetics with continuous controlled release of SN38. The cellular uptake study also showed that SN38-loaded targeted liposomes were efficiently taken up into MCF7 cells. The results of the pharmacokinetic studies revealed that SN38-loaded targeted liposomes had a slightly increased half-life and MRT and decreased AUC and C_{max}, suggesting that retention was achieved but the exposure of SN38 significantly decreased. IVIS images indicated that SN38-loaded targeted liposomes selectively targeted MCF7 tumors. Moreover, the toxicity data suggested that the decrease in Plt was significantly ameliorated by SN38-loaded targeted liposomes, and diarrhea was not observed in BALB/c mice. In summary, SN38-loaded targeted liposomes could be a good candidate for application in human breast cancer.

Acknowledgment

This work was supported by the Ministry of Science and Technology, Taipei, Taiwan under grant MOST 105-2320-B-037-012.

Disclosure

The authors report no conflicts of interest in this work.

References

1. Omura M, Torigoe S, Kubota N. SN-38, a metabolite of the camptothecin derivative CPT-11, potentiates the cytotoxic effect of radiation in human colon adenocarcinoma cells grown as spheroids. *Radiother Oncol*. 1997;43:197–201.
2. Meyer-Losic F, Nicolazzi C, Quinonero J, et al. DTS-108, a novel peptidic prodrug of SN38: in vivo efficacy and toxicokinetic studies. *Clin Cancer Res*. 2008;14:2145–2153.
3. Abigerges D, Chabot GG, Armand JP, Hérait P, Gouyette A, Gandia D. Phase I and pharmacologic studies of the camptothecin analog irinotecan administered every 3 weeks in cancer patients. *J Clin Oncol*. 1995;13:210–221.
4. Mi Z, Burke TG. Differential interactions of camptothecin lactone and carboxylate forms with human blood components. *Biochemistry*. 1994;33:10325–10336.
5. Huang Q, Wang L, Lu W. Evolution in medicinal chemistry of E-ring-modified camptothecin analogs as anticancer agents. *Eur J Med Chem*. 2013;63:746–757.
6. Thakur R, Sivakumar B, Savva M. Thermodynamic studies and loading of 7-ethyl-10-hydroxycamptothecin into mesoporous silica particles MCM-41 in strongly acidic solutions. *J Phys Chem B*. 2010;114:5903–5911.
7. Zunino F, Pratesi G. Camptothecins in clinical development. *Expert Opin Investig Drugs*. 2004;13:269–284.
8. Sapra P, Zhao H, Mehlig M, et al. Novel delivery of SN38 markedly inhibits tumor growth in xenografts, including a camptothecin-11-refractory model. *Clin Cancer Res*. 2008;141:888–896.
9. Garcia-Carbonero R, Supko JG. Current perspectives on the clinical experience, pharmacology, and continued development of the camptothecins. *Clin Cancer Res*. 2002;8:641–661.
10. Bala V, Rao S, Boyd BJ, Prestidge CA. Prodrug and nanomedicine approaches for the delivery of the camptothecin analogue SN38. *J Control Release*. 2013;172:48–61.
11. Kurzrock R, Goel S, Wheler J, et al. Safety, pharmacokinetics, and activity of EZN-2208, a novel conjugate of polyethylene glycol and SN38, in patients with advanced malignancies. *Cancer*. 2012;118:6144–6151.
12. Koizumi F, Kitagawa M, Negishi T, et al. Novel SN-38-incorporating polymeric micelles, NK012, eradicate vascular endothelial growth factor-secreting bulky tumors. *Cancer Res*. 2006;66:10048–10056.
13. Hamaguchi T, Doi T, Eguchi-Nakajima T, et al. Phase I study of NK012, a novel sn-38-incorporating micellar nanoparticle, in adult patients with solid tumors. *Clin Cancer Res*. 2010;16:5058–5066.
14. Alliance for Clinical Trials in Oncology. Liposomal SN-38 in treating patients with metastatic colorectal cancer. Available from: https://clinicaltrials.gov/ct2/show/NCT00311610. NLM identifier: NCT00311610. Accessed March 13, 2018.
15. Ebrahimnejad P, Dinarvand R, Jafari MR, Tabasi SA, Atyabi F. Characterization, blood profile and biodistribution properties of surface modified PLGA nanoparticles of SN-38. *Int J Pharm*. 2011;406:122–127.
16. Williams CC, Thang SH, Hantke T, et al. RAFT-derived polymer–drug conjugates: poly(hydroxypropylmethacrylamide) (HPMA)-7-ethyl-10-hydroxycamptothecin (SN-38) conjugates. *ChemMedChem*. 2012;7:281–291.
17. Sayari E, Dinarvand M, Amini M, et al. MUC1 aptamer conjugated to chitosan nanoparticles, an efficient targeted carrier designed for anticancer SN38 delivery. *Int J Pharm*. 2014;473:304–315.
18. Vangara KK, Liu JL, Palakurthi S. Hyaluronic acid-decorated PLGA-PEG nanoparticles for targeted delivery of SN-38 to ovarian cancer. *Anticancer Res*. 2013;33:2425–2434.
19. Du Y, Zhang W, He R, et al. Dual 7-ethyl-10-hydroxycamptothecin conjugated phospholipid prodrug assembled liposomes with in vitro anticancer effects. *Bioorg Med Chem*. 2017;25:3247–3258.
20. Basel TM, Balivada S, Shrestha BT, et al. A cell-delivered and cell-activated SN38-dextran prodrug increases survival in a murine disseminated pancreatic cancer model. *Small*. 2012;8:913–920.
21. Cardillo TM, Govindan SV, Sharkey RM, et al. Sacituzumab govitecan (IMMU-132), an anti-trop-2/SN-38 antibody-drug conjugate: characterization and efficacy in pancreatic, gastric, and other cancers. *Bioconjug Chem*. 2015;26:919–931.
22. Ying T, Wen Y, Dimitrov DS. Precision immunomedicine. *Emerg Microbes Infect*. 2017;6:e25.
23. Sahota S, Vahdat LT. Sacituzumab govitecan: an antibody-drug conjugate. *Expert Opin Biol Ther*. 2017;17:1027–1031.
24. Atyabi F, Farkhondehfai A, Esmaeili F, Dinarvand R. Preparation of PEGylated nano-liposomal formulation containing SN-38: in vitro characterization and in vivo biodistribution in mice. *Acta Pharm*. 2009;59:133–144.
25. Zwicke GL, Mansoori GA, Jeffery CJ. Utilizing the folate receptor for active targeting of cancer nanotherapeutics. *Nano Reviews*. 2012;3:18496.
26. Charles River Laboratories [website on the Internet]. Available from: http://www.criver.com. Accessed March 13, 2018.
27. Roger E, Lagarce F, Benoit JP. Development and characterization of a novel lipid nanocapsule formulation of SN38 for oral administration. *Eur J Pharm Biopharm*. 2011;79:181–188.
28. Lin CH, Al-Suwayeh SA, Hung CF, Chen CC, Fang JY. Camptothecin-loaded liposomes with α-melanocyte-stimulating hormone enhance cytotoxicity toward and cellular uptake by melanomas: an application of nanomedicine on natural product. *J Tradit Complement Med*. 2013;3:102–109.
29. Santi DV, Schneider EL, Ashley GW. Macromolecular prodrug that provides the irinotecan (CPT-11) active-metabolite SN-38 with ultralong half-life, low C_{max}, and low glucuronide formation. *J Med Chem*. 2014;57:2303–2314.
30. Li J, Wang X, Zang T, et al. A review on phospholipids and their main applications in drug delivery systems. *Asian J Pharm Sci*. 2015;10:81–98.
31. Vuković L, Khatib FA, Drake SP, et al. Structure and dynamics of highly PEG-ylated sterically stabilized micelles in aqueous media. *J Am Chem Soc*. 2011;133:13481–13488.
32. Fu Y, Kao WJ. Drug release kinetics and transport mechanism of non-degradable and degradable polymeric delivery system. *Expert Opin Drug Deliv*. 2010;7:429–444.
33. Modi S, Anderson BD. Determination of drug release kinetics from nanoparticles: overcoming pitfalls of the dynamic dialysis method. *Mol Pharm*. 2013;10:3076–3089.
34. Lombardo D, Calandra P, Barreca D, Magazù S, Kiselev MA. Soft interaction in liposome nanocarriers for therapeutic drug delivery. *Nanomaterials (Basel)*. 2016;6:E125.
35. Elbayoumi TA, Torchilin VP. Enhanced cytotoxicity of monoclonal anticancer antibody 2C5-modified doxorubicin-loaded PEGylated liposomes against various tumor cell lines. *Eur J Pharm Sci*. 2007;32:159–168.
36. Klymchenko AS, Kreder R. Fluorescent probes for lipid rafts: from model membranes to living cells. *Chem Biol*. 2014;21:97–113.
37. Zylberberg C, Matosevic S. Pharmaceutical liposomal drug delivery: a review of new delivery systems and a look at the regulatory landscape. *Drug Deliv*. 2016;23:3319–3329.
38. Paliwal SR, Paliwal R, Agrawal GP, Vyas SP. Liposomal nanomedicine for breast cancer therapy. *Nanomedicine (Lond)*. 2011;6:1085–1100.
39. Goren D, Horowitz AT, Tzemach D, Tarshish M, Zalipsky S, Gabizon A. Nuclear delivery of doxorubicin via folate-targeted liposomes with bypass of multidrug-resistance efflux pump. *Clin Cancer Res*. 2000;6:1949–1957.
40. Chen H, Ahn R, van den Bossche J, Thompson DH, O'Halloran TV. Folate-mediated intracellular drug delivery increases the anticancer efficacy of nanoparticulate formulation of arsenic trioxide. *Mol Cancer Ther*. 2009;8:1955–1963.

41. Pal A, Khan S, Wang YF, et al. Preclinical safety, pharmacokinetics and antitumor efficacy profile of liposome-entrapped SN-38 formulation. *Anticancer Res*. 2005;25:331–341.
42. Nishikawa K, Arai H, Inoue K. Scavenger receptor-mediated uptake and metabolism of lipid vesicles containing acidic phospholipids by mouse peritoneal macrophages. *J Biol Chem*. 1990;265:5226–5231.
43. Funato K, Yoda R, Kiwada H. Contribution of complement system on destabilization of liposomes composed of hydrogenated egg phosphatidylcholine in rat fresh plasma. *Biochim Biophys Acta*. 1992; 1103:198–204.
44. Harashima H, Sakata K, Funato K, Kiwada H. Enhanced hepatic uptake of liposomes through complement activation depending on the size of liposomes. *Pharm Res*. 1994;11:402–406.
45. Immordino ML, Dosio F, Cattel L. Stealth liposomes: review of the basic science, rationale, and clinical applications, existing and potential. *Int J Nanomedici*ne. 2006;1:297–315.
46. Rich TA, Kirichenko AV. Camptothecin schedule and timing of administration with irradiation. *Oncology*. 2001;15:37–41.
47. Araki E, Ishikawa M, Iigo M, Koide T, Itabashi M, Hoshi A. Relationship between development of diarrhea and the concentration of SN-38, an active metabolite of CPT-11, in the intestine and the blood plasma of athymic mice following intraperitoneal administration of CPT-11. *Jpn J Cancer Res*. 1993;84:697–702.